Production of Hydronium Ion $(H_3O)^+$ and Protonated Water Clusters $(H_2O)_nH^+$ after Energetic Ion Bombardment of Water Ice in Astrophysical Environments

R. Martinez[1,2 *], A.N. Agnihotri[1,a], Ph. Boduch[1], A. Domaracka[1], D. Fulvio[3], G. Muniz[1,b], M.E. Palumbo[4], H. Rothard[1], G. Strazzulla[4]

[1]Centre de Recherche sur les Ions, les Matèriaux et la Photonique, CIMAP, Normandie Univ, ENSICAEN, UNICEN, CEA, CNRS, CIMAP, 1400 Caen, France

[2]Departamento de Física, Universidade Federal do Amapá, Brazil

[3]Departamento de Física, Pontificia Universidade Catolica do Rio de Janeiro, Brazil

[4]INAF-Osservatorio Astrofisico di Catania, Via S. Sofia 78, 95123 Catania, Italy

[a]*now at: Indian Institute of Technology Delhi, India*

[b]*now at: Institute of Physics, University of São Paulo, Brazil*

Abstract

Water ice exists on many objects in space. The most abundant icy species, among them water, are present in the icy satellites of the outer Solar System giant planets. The nucleus of comets, which is mainly composed of water ice, is another example of its abundance. In the interstellar medium (ISM), ice mantles, formed by molecular species sticking on dust grains, consist mainly of water ice. All these objects are exposed to ionizing radiation like ions, UV photons and electrons. Sputtering of atoms, molecules, ions and radicals from icy surfaces may populate and maintain exospheres of icy objects in the Solar System. In other respect, ionized hydrides such as OH^+, H_2O^+ and H_3O^+ have been detected in the gas-phase in star forming regions. Interactions with cosmic rays could be an additional explanation to the current models for the formation of those species. In fact, laboratory simulations showed that the main components of the sputtered ionic species from water ice are oxygen hydrides. In this work, water ice targets were irradiated at several temperatures (10-200 K) by 90 keV O^{6+} ions, yielding an electronic stopping power of about 12 eV/Å, when the nuclear stopping power is comparable to the electronic stopping power. Sputtering of secondary ions after bombardment of the ice target was analyzed by time-of-flight mass spectrometry (TOF-SIMS). Besides hydrogen ions (H^+, H_2^+, H_3^+), also O^+, O^{2+}, OH^+, $(H_2O)^+$ and clusters of $(H_2O)_nH^+$ with n = 1-8 are emitted. Our results show a progressive yield decrease with increasing temperature of all of the detected species. This is related to the structure of the ice: the ionic sputtering yield for crystalline ice is much lower than for an amorphous ice. For instance, amorphous ice at 10 K exhibits a yield of the order of $2x10^{-6}$ secondary $(H_2O)_nH^+$ hydride ions/projectile (with n=1-8).

When increasing the temperature towards the phase transition to crystalline ice, the yields decrease by about one order of magnitude.

* Corresponding author:
Rafael Martinez
e-mail: rafael.mr@unifap.br
Tel: +55 96 98401-7043

1. Introduction

Hydrides are molecules containing only one heavy element atom (C, N, O etc.) with one or more hydrogen atoms. They are among the simplest molecules that are firstly formed and then are at the basis of the chemical evolution in the interstellar medium of our and other galaxies (for a review see Gerin et al. 2016). Hydrides are also present and widely observed in the solid and/or in the gas phase in almost all of the objects in the Solar System (Lis et al. 2009, Bockelée-Morvan et al. 1998).

The oxygen containing (OH, H_2O, OH^+, H_2O^+, H_3O^+) are among the most abundant hydrides and play a fundamental role in the chemical composition and evolution of the tenuous atmospheres (exospheres) of many objects that are dominated by water ice such as the icy satellites of the giant planets in the outer Solar System (see e.g. Cassidy et al. 2007). The surfaces of those objects are bombarded by intense fluxes of magnetospheric ions, mostly H, and multicharged O and S and electrons that are believed to be among the most important agents driving the chemical evolution of those surfaces. In addition Hydrogen, helium and oxygen ions are the most abundant in the Solar Wind. In particular ion bombardment sputters atoms, molecules, ions and radicals (mostly oxygen hydrides) from the surface so populating and maintaining their exospheres (Strazzulla 2011; Plainaki et al. 2015). Obviously the above hypothesis is based on laboratory experiments that have, so far, mostly concentrated on the measurements of the sputtering yields, energy distributions and angular dependence of the neutrals (H_2O, OH, O_2H etc) which are the most abundant species sputtered by particle and electron bombardment of ice (e.g. Johnson et al. 2004).

Much less laboratory results are available on the production of secondary ions following the interaction between energetic particles and ice (see Collado et al. 2004; Farenzena et al. 2006; de Barros et al. 2011). These papers focus on the effects of fast ions losing their energy within the irradiated ice in the electronic regime, i.e. when the electronic stopping power (S_e) is significantly higher than the nuclear one (S_n). In the current paper we wish to give a further contribution to the field by reporting the results of a series of experiments on the production of secondary ions after 90 keV O^{6+} bombardment of water ice. In such conditions, the nuclear stopping power is comparable to the electronic stopping power. The projectiles energy loss is either due to inelastic collisions (excitation or ionization, S_e) or elastic collisions (S_n). Sputtering yields, to name an example, were found to scale with a certain power of S_e. The scaling law of the latter with S_n may be different. The experiments were performed in the wide range ice temperature (10-200 K), which are of astrophysical interest.

The results of the present work demonstrate the production of several ions and in particular, the hydronium ion $(H_3O)^+$ and protonated water clusters $(H_2O)_nH^+$. The production yields show a

dependence on the structure of the ice. Crystalline ices exhibit yields about one order of magnitude lower than amorphous ices.

The experiments are discussed in view of their relevance in some astrophysical scenarios like planetary ices and interstellar grains. In the former, the presence of water ice is abundant, e. g. on the surface of the icy moons in the outer Solar System. This is the case of the main satellites of Jupiter, Saturn, Uranus and Neptune (e.g. Schmitt et al. 1998), where water ice can exhibit several structures (Grundy et al. 1999). For instance, according to Hansen and McCord (2004), the three Jovian icy satellites Europa, Callisto, and Ganymede may exhibit amorphous, crystalline or both structures. Likewise important is the presence of the hydronium ion in the coma of comets dominated by water in their icy phase (Balsiger et al. 1995; Nordholt et al. 2003). Furthermore, in dense clouds of the ISM, ice mantles formed on dust grains also suffer intense low-energy cosmic rays and UV photons bombardment, undergoing physical and chemical changes. In addition to these processes the structure of ice mantles can be transformed, for instance, from amorphous to crystalline when protostellar objects heat their circumstellar envelopes (e.g. Dartois and D'Hendecourt, 2001; Schegerer and Wolf, 2010).

2. Experimental procedures

The experiments were performed at the low energy ion beam facility ARIBE of GANIL (Grand Accélérateur National d'Ions Lourds) in Caen, France, with 90 keV O^{6+} ions impacting on water ices of various thicknesses deposited and irradiated at temperatures ranging from 10 to 200 K. The temperature of the Cu substrate was controlled using a Lake Shore Model 336 Cryogenic Temperature Controller. The experimental set-up (AODO) contains a cryo-cooled Cu substrate in an ultrahigh vacuum chamber (base pressure $<10^{-8}$ mbar). The water ice targets were deposited on this substrate *in situ* and irradiated with a pulsed (~10 ns) ion beam (90 keV O^{6+}). The secondary ions emitted from the targets were analyzed by using a Recoil Ion Momentum Spectrometer. A schematic view of the XY-TOF-SIMS setup is shown in Figure 1. The details of the set-up have been described elsewhere (Hijazi et al. 2012, Allodi et al. 2013).

The water sample was stored in a glass tube connected to a pre-chamber. The glass tube was evacuated several times after the water sample was frozen using a liquid nitrogen bath. The pre-chamber was purged with water vapor several times to remove any residual gas. To prepare the ice targets, water vapor was introduced into the experimental chamber using a fine valve to obtain a stable flow in the chamber. The thickness of the ice targets were calculated using the pressure in the chamber and the time duration of the deposition; such a technique was calibrated many times during

the large number of experiments conducted by using the same technique of deposition by measuring, a posteriori, the column density of the deposited water ice layers by IR spectroscopy (see e.g. Ding et al. 2013) or, recently, directly with a quartz micro-balance during deposition. The thickness of the irradiated samples was always larger than the penetration depth of the incoming ions (from 2 μm to ~10 μm).

The ion beam defined with a set of three collimators was pulsed using a parallel plate deflector with a small aperture in front. The pulse also provides a START signal for data acquisition. The applied electrostatic field extracts the secondary ions, sputtered from the targets. After passing the field free drift region, the ions are detected by a position-sensitive Micro-Channel-Plate (MCP) detector. The MCP signal provides the STOP signal. Using these START and STOP signals, a time of flight spectrum is obtained which, after calibration, provides the mass spectrum for secondary ion sputtering from the ice targets.

Each pulse lasts 10 ns and is repeated every 100 microseconds. Usually, the data acquisition time needed for each sample is of the order of one hour. The flux of the ion beam has been estimated to be about 10^5 ions cm^{-2} s^{-1}. This corresponds to an ion fluence (after 1 hour) of about $3.6x10^8$ ions cm^{-2}, low enough to not significantly alter the structure and/or the chemical composition of the irradiated layers (Allodi et al 2013).

3. Results

A first set of experiments has been performed by depositing water ice samples on the cooled Cu substrate at 10 K. After deposition, secondary ion mass spectra were collected with the pulsed beam. The results are shown in the upper panel of Figure 2. A large variety of different secondary ions are emitted. Those that are detectable are labeled in the figure: evident are hydrogen ions (H^+, H_2^+, H_3^+), O^+, O^{2+}, OH^+, $(H_2O)^+$ and clusters of $(H_2O)_nH^+$ with n=1-8 (in Figure 2 only those with n up to 4 are shown).

The same sample has then been warmed up to 50 K, the cycle of measurement repeated and the sample further warmed up to 100 K for a new measurement. The results are shown in the medium and bottom panels of Figure 2. A progressive decrease with increasing temperature of all of the detected peaks is quite evident as will be quantified later in this paper.

To verify if the observed effect (i.e. the decrease of the production efficiency with temperature) is simply due to the "aging" of the surface that, as said, has not been refreshed, we performed experiments with fresh ice layers at different temperatures. In all of the cases the thickness of the fresh layer is larger than the penetration depth of the incoming ions. The results are shown in Figure 3. The top panel presents the case of a layer deposited at 10 K then, from top to the bottom, the spectra obtained for the ice deposited at increasing temperatures (up to 120 K) are shown. We can see that the trend observed in Figure 2 is confirmed: the efficiency clearly decreases with increasing temperature. The second spectrum from the bottom refers to a temperature of 200 K at which all of the water molecules are sublimated and the spectrum can then be considered as a background. The last spectrum (at 10 K) has been obtained with a fresh water layer for a further confirmation of the effect.

It still remains to clarify if the decrease of the production efficiency with the temperature is connected with the structure of the ice (amorphous vs. crystalline). It is in fact very well known that the structure of water (and other ices, too) strongly depends on the temperature at which it is formed. Water ice is amorphous if deposited at low temperature (10-30 K), or crystalline if the deposition temperature is higher (140-150 K) (Palumbo 2006, Bossa et al. 2012). If deposited at intermediate temperatures the structure can be regarded as a combination of amorphous and crystalline ice with the amorphous fraction increasing with decreasing T. The crystalline structure is stable against temperature cycling, i.e. an ice target formed at 150 K and cooled down to 10 K preserves its crystalline structure. On the other hand, an amorphous ice layer formed at low temperature and heated to 150 K rapidly (in a few seconds) is transformed into a crystal (Schmitt et al. 1988, Baragiola 2003). Thus, we have prepared crystalline ice samples by depositing H_2O at 10 K (amorphous), heating them to 150 K (transition amorphous to crystal) and cooling them down to

10 K. The target has been irradiated with the oxygen beam as done in the already described experiments yielding the secondary ion mass spectra shown in Figure 4. It is quite evident that the production efficiency for crystalline ice is much lower than for an amorphous ice. Spectra acquired at increasing temperatures confirm the result.

As discussed in Dartois et al. (2015) and Rothard et al. (2017) (and references therein), ion bombardment of crystalline ice at low temperature causes a progressive damage in the crystalline structure, eventually up to complete amorphisation. However, as said above, the ion fluences used in the experiments described here are very low and the damage is negligible.

To quantify the results we have calculated the yields (secondary ions produced per impinging projectile ion) from the knowledge of the fluence of incoming projectile ions (ions/cm^2) and the measured counts of emitted secondary ions. The results are shown in Figure 5, where we report the data for the most abundant secondary ion $(H_3O)^+$ and for the total amount of clusters $(H_2O)_nH^+$ (n=1-8). Amorphous ice at 10 K exhibits a yield of the order of $2x10^{-6}$ secondary hydride ions/projectile. We note that about 50% of them correspond to n=1. With increasing temperature the yields decrease by about one order of magnitude. It is also clear that in the case of crystalline ice the yields are lower at any temperature.

In the same figure we have also reported the results for the total amount of hydrogen ions (only for the experiments when fresh ice layers where deposited before the measurement at a given temperature). The sum of emitted hydrogen ions (H^+, H_2^+, H_3^+) amounts to a value of about 10^{-4} and does not depend on T. This has, however, to be taken with care since hydrogen is always emitted from the walls of the chamber being present as an unavoidable contaminant. This is also clearly seen in Fig. 3 (T=200 K), where the signal of H^+ and H_2^+ is still evident, even if not that strong.

To verify that the yields measured for hydronium ions are not influenced by residual impurities adsorbed on the walls of the chamber where incoming energetic ions could hit, we have performed selected experiments with deuterated water at 10 K. The results are shown in Figure 6 where it is clearly demonstrated that the production yields are, within the error, the same as for the two isotopologues, thus excluding significant chamber contamination.

4. Discussion

The results described in this work add a piece of information to what was already known: the production yields of oxygen hydride secondary ions depend on the structure of the ice. Crystalline ice exhibits yields one order of magnitude lower than amorphous ice at the same temperature.

As said, there are only a few experimental data available on the measurements of the production yields of secondary ions from ion bombarded ice (Collado et al. 2004, Farenzena et al. 2006; de Barros et al. 2011). De Barros et al. (2011) presented data obtained by using N_2^+ ions at energies between 0.5 and 1.7 MeV and temperatures between 15 and 200 K. Their absolute values of the production yields of secondary ions have been obtained by scaling the measured ion counts to the absolute yields given by Collado et al. (2004) for 0.81 MeV N^+ ions colliding with water ice at 80 K. The results obtained by de Barros et al. (2011) are qualitatively similar to those here presented: the yields decrease with increasing T and most of the emitted secondary ions are $(H_2O)_nH^+$ clusters.

A direct comparison between the results presented in this work and previous results is not straightforward. In fact previous experiments (i.e. Collado et al. 2004, Farenzena et al. 2006; de Barros et al. 2011) investigated the effects of ion bombardment in the electronic regime that is when the electronic stopping power is significantly higher than the nuclear stopping power. Here we have studied the effects induced by 90 keV O^{6+} ions. In this case the electronic stopping power is comparable to the nuclear stopping power (as estimated by SRIM code, Ziegler et al. 2013). We notice that the absolute secondary yields reported in previous papers are about two or three orders of magnitude higher than the ones found in the present study. Such a big difference could be related to the different stopping powers of the used projectiles (often given in eV/Å). Indeed, de Barros et al. (2011) suggest that the secondary ion production yields scale with the third power of the electronic energy loss of the projectiles (kinetic energy lost by electronic excitations and ionizations) stopping, S_e^3. They used projectiles with electronic stopping powers in the range of 40-90 eV/Å, whereas the ions we used 90 keV O^{6+} have an electronic stopping power in water ice of about 12 eV/Å. This would correspond to a production yield 40-400 times lower, not enough to reconcile the two sets of experiments. Furthermore, Collado et al. (2004) noticed that there are indications that emission of the $(H_2O)_nH^+$ disappears for an electronic energy loss lower than 20 eV/ Å. Here, we have been able to measure the yields also for electronic energy loss as low as 12 eV/ Å when the nuclear stopping power is comparable to the electronic stopping power.

For insulators like water ice, inelastic (electronic) sputtering is several orders of magnitude more efficient than expected for elastic sputtering at comparable energy loss. Total sputtering yields also include contributions related to nuclear stopping power. With multiply charged ions at relatively low velocities, as in our case, also potential sputtering may occur. This sputtering process is

characterized by a strong dependence of the observed sputtering yields on the charge state of the impinging ion. The contribution of all these interactions may make the sputtering process more complex than previously thought. Precisely, in this regard, the ion/neutral sputtering ratio may also present some variations, mainly at relative low projectile velocities. Consequently our opinion is that the dependence of the secondary ion production yields on the total stopping power and, in particular, the contribution of the nuclear stopping power is more complex than suggested so far and needs further experiments to be fully understood.

Furthermore, sputtered particles are mostly emitted as neutrals, in the form of molecules and clusters. The dependence of Y with Se depends on the excitation processes that are needed for electronic sputtering (Brown, et al. 1982, Johnson, et al. 1982). Concerning ion sputtering, in some cases, the cluster yields Y(n) follow a power law $Y(n) \sim n^{\delta}$, in other cases, an exponential law $Y(n) \sim \exp(n)$ is observed. Possible mechanisms for cluster emission include the emission of preformed species as single entities after impact following a collective phenomenon such as a shock wave. The observed power law dependence is a hint for such a collective mechanism. Exponential laws in contrast reflect "statistical processes" like (in-flight) fragmentation or agglomeration after strong electronic excitation leading to the formation of a local plasma (Prudence, et al. 2019).

The results obtained so far might be of interest in many astrophysical scenarios. As a general remark we believe that an important parameter to know in view of astrophysical applications is the ratio between the amount of sputtered secondary ions and the sputtering yield of neutrals (this parameter in our case of water ice scales with a very well known parameter on S_e^2, see e.g. Baragiola et al. 2003). The above findings imply that such a ratio varies of several orders of magnitude depending on the mass and energy of the projectile. As an example Collado et al. find that the ratio is about $5x10^{-4}$ for 0.81 MeV N^+ at 80 K and we estimate that it is on the order of $2x10^{-8}$ for 90 keV O^{6+} at 80 K.

4.1 Planetary ices

The experiments here presented explore the production of the hydronium ion $(H_3O)^+$ and clusters $(H_2O)_nH^+$ after energetic ion bombardment of water ice at different temperatures, able to cover the range of temperatures spanned by ice surfaces when moving outward the Solar System until the interstellar medium. The results of the present work are therefore of interest for the outer Solar System, where water ice represents the most abundant icy species, such as in the case of the main satellites of Jupiter, Saturn, Uranus and Neptune (e.g. Schmitt et al. 1998) and the so called trans-Neptunian objects (see for instance Barucci et al. 2008). Moreover, interestingly enough, the

hydronium ion has been observed in the coma of comets dominated by water in their icy phase (Balsiger et al. 1995; Nordholt et al. 2003). In other words, the effects here reported on the yields of ion emission depending on the structure of the ice (crystalline vs amorphous) are relevant in the outer Solar System. In this context, we point out that the phase changes are those induced by thermal (e.g. Mastrapa et al. 2013) and non-thermal processes as discussed above.

Besides comets, another interesting example of the applicability of our results is represented by the icy satellites in the outer Solar System, where surficial water ice can exhibit a variety of structures (Grundy et al. 1999). This is for instance the case of the three Jovian icy satellites Europa, Callisto, and Ganymede which exhibit different structures: ice is mostly amorphous on the surficial layers of Europa (where the temperature is lower) and crystalline on Callisto (which has higher temperature), while both structures are found on Ganymede (Hansen and McCord 2004). This means that the results presented in the current work will be of great interest for the analysis and characterization of the constituents of the tenuous atmospheres of such satellites (Coustenis et al. 2010), generated by the energetic ions (O^{n+}, S^{n+} and H^{+}) and electrons coming from the Jovian magnetosphere and colliding with the ice present on the surface of the satellites (e.g., Johnson 1990; Strazzulla and Johnson 1991; Cooper et al. 2001). In fact, even though to date these atmospheres are not so well characterized, one of the main goals of the upcoming JUpiter ICy moons Explorer (JUICE) mission by ESA is to provide a detailed investigation of Ganymede, Europa, and Callisto (Grasset et al. 2013). In this view, their atmospheres will be extensively studied and characterized mainly by the Particle Environment Package (PEP), the Sub-millimeter Wave Instrument (SWI), and the Gravity & Geophysics of Jupiter and Galilean Moons (3GM) instrument onboard JUICE. We think that the results presented in the current work will strongly contribute in the interpretation and understanding of these data.

4.2 Interstellar grains

Ice mantles form on dust grains in dense clouds because of the sticking of atomic and molecular species from the gas phase that may also react on the grain itself. The major observed constituent of ices in the interstellar medium is water, making up 60–70% of the ices (Tielens et al. 1982; Boogert et al. 2015). In quiescent clouds water ice is amorphous and it is formed at low temperature by surface reaction of O (and/or O_2 and/or O_3) and H (or OH) or even of H_2 with OH on the cold refractory dust as experimentally evidenced (Ioppolo et al. 2008, Oba et al. 2009, Mokrane et al. 2009, Dulieu et al. 2010, Oba et al. 2012). Dense clouds are the site of star formation and during this process ice mantles and grains undergo physical and chemical changes driven by energetic processing (i.e. bombardment by low-energy cosmic rays and UV photons) and thermal annealing.

Thus, for example, the structure of ice mantles can be transformed from amorphous to crystalline when protostellar objects heat their circumstellar envelopes (e.g. Dartois and D'Hendecourt, 2001; Schegerer and Wolf, 2010). On the other hand, energetic processing of crystalline ice at temperature lower than 70 K causes the ice amorphization (e.g. Kouchi and Kuroda 1990; Baratta et al. 1991; Strazzulla et al. 1992; Moore et al. 1992; Leto and Baratta 2003; Dartois et al. 2015).

Ionized hydrides such as OH^+, H_2O^+ and H_3O^+ have been detected in the gas-phase in star forming regions (e.g. Wootten et al. 1991; van der Tak et al. 2006; Hollenbach et al. 2012; Benz et al. 2010, 2016). According to current models, OH^+, H_2O^+ and H_3O^+ form in the gas phase after ion-neutral reactions via ionization of atomic H and molecular H_2 induced by cosmic rays (e.g. Hollenbach et al. 2012). The experimental results here discussed show that the interaction of cosmic rays with ice grain mantles could be an additional process which contributes to the formation of ionized species. At present it is not possible to quantify the contribution of the interaction of cosmic rays with icy mantles to the production of ionized hydrides in dense clouds. To this end more experimental results are necessary.

5. Conclusion

Water ice films of various thicknesses were bombarded by 90 keV O^{6+} ions at several temperatures, ranging from 10 to 200 K. The sputtered particles were analyzed by TOF-SIMS, which mainly detected the hydronium ion $(H_3O)^+$ and $(H_2O)_nH^+$ clusters. Oxygen hydrides are important in the Solar System since they form e.g. the exospheres of icy moons of the giant planets. In addition, they are of particular interest for astrochemistry, as they are the basic building blocks of the chemical networks in both diffuse and dense clouds (Lis et al. 2009).

Our results confirmed the dependence of sputtering yields of ionic species with the water ice structure: on the whole, amorphous ice, deposited at low temperature (10-30 K), exhibits high sputtering yields. On the other hand, crystalline ice, deposited at high temperature (140-150 K) or deposited at low temperature and heated up to 150 K, shows low sputtering yields. Such an effect was not noticed before nor has been investigated for the sputtering yields of the neutrals that, as said, are order of magnitudes higher than those of the ionized species.

As a final remark we notice that both cationic and anionic species are emitted after ion bombardment. From the astrochemical point of view, both are important. Unfortunately our experimental set-up in its present configuration did not allow us to detect anionic species.

Acknowledgements

We thank the staff of CIMAP and GANIL and among them all in particular T. Been, C. Feierstein, J.M. Ramillon, F. Ropars and P. Rousseau. We gratefully acknowledge funding from INSERM-INCa (Grant BIORAD), Région Normandie Fonds Européen de Développement Régional - FEDER Programmation 2014-2020. This work was also supported by the Brazilian agencies CNPq (INEspaço and Science without Borders) and FAPERJ, and by the Italian Ministero dell' Istruzione, dell' Università e della Ricerca through the grant Progetti Premiali 2012-iALMA (CUP C52I13000140001). GS was supported by the Italian Space Agency (ASI 2013-056 JUICE Partecipazione Italiana alla fase A/B1) and by the European COST Action CM1401-Our Astrochemical History.

References

Allodi, M. A., and 21 colleagues, 2013, **Complementary and Emerging Techniques for Astrophysical Ices Processed in the Laboratory**, Sp. Sci. Rev. 180, 101

Balsiger, H., Altwegg, K., Geiss, J., 1995, **D/H and $^{18}O/^{16}O$ ratio in the hydronium ion and in neutral water from in situ ion measurements in comet Halley**, Journal of Geophysical Research, 100, 5827

Baragiola, R. A., 2003, **Water ice on outer solar system surfaces: Basic properties and radiation effects**, Planet. Space Sci., 51, 953

Baragiola, R. A., Vidal, R. A., Svendsen, W., Schou, J., Shi, M., Bahr, D. A., Atteberrry, C. L., 2003, **Sputtering of water ice**, Nucl Instr Meth B 209, 294

Baratta, G. A., Leto, G., Spinella, F., Strazzulla, G., & Foti, G. 1991, **A comparison of ion irradiation and UV photolysis of CH_4 and CH_3OH**, A&A, 252, 421

de Barros, A. L. F., Farenzena, L. S., Andrade, D. P. P., da Silveira, E. F., Wien K., 2011, **Secondary Ion Emission from Water Ice at 10 - 130 K Induced by MeV N^{2+} Ions**, J. Phys. Chem. C, 115, 12005

Barucci M. A., Boehnhardt H., Cruikshank D. P., and Morbidelli A. (eds.), **The Solar System Beyond Neptune**, University of Arizona Press, Tucson, 2008

Benz, A. O., Bruderer, S., van Dishoeck, E. F., et al. 2010, ***Herschel*/HIFI observations of high-*J* CO transitions in the protoplanetary nebula CRL 618***, A&A, 521, L3

Benz, A. O., Bruderer, S., van Dishoeck, E. F., et al. 2016, **Water in star-forming regions with *Herschel* (WISH)**, A&A, 590, A105

Bockelée-Morvan, D., Gautier, D., Lis, D. C., Young, K., Keene, J., Phillips, T. G., Owen, T., Crovisier, J., Goldsmith, P. F., Bergin, E. A., Despois, D., Wootten, A. 1998, **Deuterated Water in Comet C/1996 B2 (Hyakutake) andIts Implications for the Origin of Comets**, Icarus 133, 147

Bossa J.-B., Isokoski K., de Valois M. S., Linnartz H., 2012, **Thermal collapse of porous interstellar ice**, A&A 545, A82

Brown W.L., et al. Nucl. Instr. And Meth. 198 (1982) 1.

Cassidy T.A., Johnson R.E., McGrath M.A., Wong M.C., Cooper J.F., 2007, **The spatial morphology of Europa's near-surface O_2 atmosphere**, Icarus 191, 755

Collado, V.M., Farenzena, L. S., Ponciano, C.R., da Silveira, E. F., Wien K., 2004, **Ion desorption from frozen H_2O irradiated by MeV heavy ions**, Surface Science 569, 149

Cooper J. F., Johnson R. E., Mauk B. H., Garret H. B. and Gehrels N., 2001, **Energetic Ion and Electron Irradiation of the Icy Galilean Satellites**, Icarus, 149, 133

Coustenis, A., Tokano, T., Burger, M.H., Cassidy, T.A., Lopes, R.M., Lorenz, R.D., Retherford, K.D., Schubert, G., 2010, **Atmospheric/Exospheric Characteristics of Icy Satellites**, Space Science Reviews 153, 155–184

Dalton, J.B., Cruikshank, D .P., Stephan, K., McCord, T.B., Coustenis, A., Carlson R.W., Coradini, A., 2010, **Chemical Composition of Icy Satellite Surfaces**, Sp. Sci. Rev. 153, 113

Dartois, E., D'Hendecourt, L., 2001, **Search for NH_3 ice in cold dust envelopes around YSOs**, Astron Astrophys, 365, 144

Dartois E., Augé B., Rothard H., Boduch P., Brunetto R., Chabot M., Domaracka A., Ding J.-J., Kamalou O., Lv X.-Y., da Silveira E. F., Thomas J.-C., Pino T., Mejia C.R., Godard M., de Barros A.L.F., 2015, **Swift heavy ion modifications of astrophysical water ice**, Nucl. Instrum. Meth. B 365, 472

Dartois, E., Augé, B., Boduch, P., et al. 2015, **Heavy ion irradiation of crystalline water ice: Cosmic ray amorphisation cross-section and sputtering yield**, A&A, 576, A125

Domingue D. L. and 21 colleagues, 2014, **Mercury's Weather-Beaten Surface: Understanding Mercury in the Context of Lunar and Asteroidal Space Weathering Studies**, Space Science Reviews 181, 121

Dulieu F., Amiaud L., Congiu E., Fillion J.-H., Matar E., Momeni A., Pirronello V. and Lemaire J. L., 2010, **Experimental evidence for water formation on interstellar dust grains by hydrogen and oxygen atoms**, A&A, 512, A30.

Farenzena, L. S., and 10 colleagues, 2005, **Electronic Sputtering Analysis of Astrophysical Ices**, Earth, Moon, Planets 97, 311

Gerin M., Neufeld D.A., Goicoechea J.R. 2016, **Interstellar Hydrides**, Ann. Rev. Astron. Astrophys. 54, 181

Grasset O. et al. 2013, **JUpiter ICy moons Explorer (JUICE): An ESA mission to orbit Ganymede and to characterise the Jupiter system**, Planetary and Space Science, 78, 1

Grundy W.M., Buie M.W., Stansberry J.A., Spencer J.R. and Schmitt B. 1999, **Near-Infrared Spectra of Icy Outer Solar System Surfaces: Remote Determination of H_2O Ice Temperatures**, Icarus 142, 536–549.

Hansen, G.B., McCord, T.B. 2004, **Amorphous and crystalline ice on the Galilean satellites: A balance between thermal and radiolytic processes**, J Geophys Res 109, E01012

Ioppolo S., Cuppen H.M., Romanzin C., van Dishoeck E. F. and Linnartz H., 2008, **Laboratory Evidence for Efficient Water Formation in Interstellar Ices**, ApJ 686, 1474.

Hijazi, H., Rothard, H., Boduch, Ph., Alzaher, I., Cassimi, A., Ropars, F., Been, T., Ramillon, J.M., Lebius, H., Ban-d'Etat, B., Farenzena, L.S., da Silveira, E.F. 2012, **Electronic sputtering: Angular distributions of (LiF)nLi+ clusters emitted in collisions of Kr (10.1 MeV/u) with LiF single crystals**, Eur. Phys, J. D: Atomic, Molecular and Optical Physics 66, 68

Hollenbach, D.; Kaufman, M. J.; Neufeld, D.; Wolfire, M.; Goicoechea, J. R. 2012, **The Chemistry of Interstellar OH+, H2O+, and H3O+: Inferring the Cosmic-Ray Ionization Rates from Observations of Molecular Ions**, The Astrophysical Journal, 754: 105

Johnson R.E., et al. Nucl. Instr. and Meth 198 (1982) 103.

Johnson R. E., 1990, **Energetic charged-particle interaction with atmospheres and surfaces**, Vol. 19 (Springer-Verlag)

Johnson R.E., Carlson R.W., Cooper J.F., Paranicas C., Moore M.H., Wong M.C., 2004, **Planet Satellites Magnetosphere**. In: Jupiter: The planet, satellites and magnetosphere. Edited by Bagenal F., Dowling T. E., McKinnon W. B. Cambridge planetary science, Vol. 1, Cambridge, UK: Cambridge University Press, ISBN 0-521-81808-7, 2004, p. 485 – 512.

Kouchi, A., & Kuroda, T. 1990, **Amorphization of cubic ice by ultraviolet irradiation**, Nature, 344, 134

Langlinay, Th., **Effets de l'irradiation des ions lourds multichargés sur des cristaux et des glaces d'intérêt astrophysique**, PhD Thesis Université de Caen Basse-Normandie, 2014 (HAL Id: tel-01098780).

Leto, G. and Baratta, G. A. 2003, **Ly-α photon induced amorphization of Ic water ice at 16 Kelvin**, A&A 397, 7

Lis D.C., Goldsmith P. F., Bergin E. A., Falgarone E., Gerin M., Roueff E., 2009, **Hydrides in Space: Past, Present, and Future**, ASP Conference Series 417, 23.

Mastrapa R.M.E., Grundy W.M., Gudipati M.S., 2013, **Amorphous and Crystalline H_2O-Ice**. In: Gudipati M.S., Castillo-Rogez J. (eds) The Science of Solar System Ices. Springer, New York

Mokrane H., Chaabouni H., Accolla M., Congiu E., Dulieu F., Chehrouri M. and Lemaire J.L., 2009, **Experimental Evidence for Water Formation Via Ozone Hydrogenation on Dust Grains at 10 K**, *ApJ* 705, L195

Moore, M.H., & Hudson, R.L. 1992, **Far-infrared spectral studies of phase changes in water ice induced by proton irradiation**, ApJ, 401, 353

Nordholt, J.E., D.B. Reisenfeld, R.C. Wiens, et al. 2003, **Deep Space 1 encounter with Comet 19P/Borrelly: Ion composition measurements by the PEPE mass spectrometer,** Geophysical Research Letters, 30, 1465

Oba Y., Miyauchi N., Hidaka H., Chigai T., Watanabe N., Kouchi A., 2009, **Formation of Compact Amorphous H_2O Ice by Codeposition of Hydrogen Atoms with Oxygen Molecules on Grain Surfaces**, ApJ 701, 464.

Oba Y., Watanabe N., Hama T., Kuwahata K., Hidaka H. and Kouchi A., 2012, **Water Formation Through a Quantum Tunneling Surface Reaction, OH + H_2, at 10 K**, ApJ 749, 67.

Palumbo M. E., 2006, **Formation of compact solid water after ion irradiation at 15 K**, A&A 453, 903.

Plainaki C., Milillo A., Massetti S., Mura A., Jia X., Orsini S., Mangano V., De Angelis E., Rispoli R., 2015, **The H_2O and O_2 exospheres of Ganymede: The result of a complex interaction between the jovian magnetospheric ions and the icy moon**, Icarus 245, 306

Porter S.B., Desch S.J., Cook J.C., 2010, **Micrometeorite impact annealing of ice in the outer Solar System**, Icarus 208, 492

Prudence C.J.A.B., et al. Low Temp. Physics 45 (2019) 590.

Schegerer, A.A., Wolf, S., 2010, **Spatially resolved detection of crystallized water ice in a T Tauri object**, A&A 517, A87

Schmitt B., Grimm R., Greenberg M., 1988, **H_2O and CO_2H_2O ices**, in Proc. 22nd Elsab Symposium on Infrared Spectroscopy in Astronomy, Salamanca, p. 213

Schmitt, B.; de Bergh, C.; Festou, M. eds. **Solar system Ices**, 1998 Astrophysics and space science library (ASSL) Series vol no 227

Shen, C.J., Greenberg, J.M., Schutte, W.A., van Dishoeck, E.F., 2004, **Cosmic ray induced explosive chemical desorption in dense clouds**, A&A 415, 203

Strazzulla G. and Johnson R. E., 1991, **Comets in the post-Halley era**, Vol. 167 (Dordrecht: Kluwer Academic Publishers ASSL Series), p. 243

Strazzulla, G., Baratta, G. A., Leto, G., & Foti, G. 1992, **Ion-Beam–Induced Amorphization of Crystalline Water Ice**, Europhys.Lett., 18, 517

Strazzulla G. 2011, **Cosmic ion bombardment of the icy moons of Jupiter**, Nucl Instr Meth B 269, 842.

Tielens A. G. G. M. and Hagen W., 1982, **Model calculations of the molecular composition of interstellar grain mantles**, A&A 114, 245

van der Tak, F. F. S., Belloche, A., Schilke, P., et al. 2006, **APEX mapping of H_3O^+ in the Sgr B2 region**, A&A,454, L99

Wootten, A., Mangum, J. G., Turner, B. E., et al. 1991, **Detection of Interstellar H_3O^+ : A Confirming Line**, ApJ, 380, L79

Ziegler J.F., Biersack J.P. and Ziegler M.D. 2013, **SRIM: The Stopping and Range of Ions in Matter** (www.srim.org)

Figures

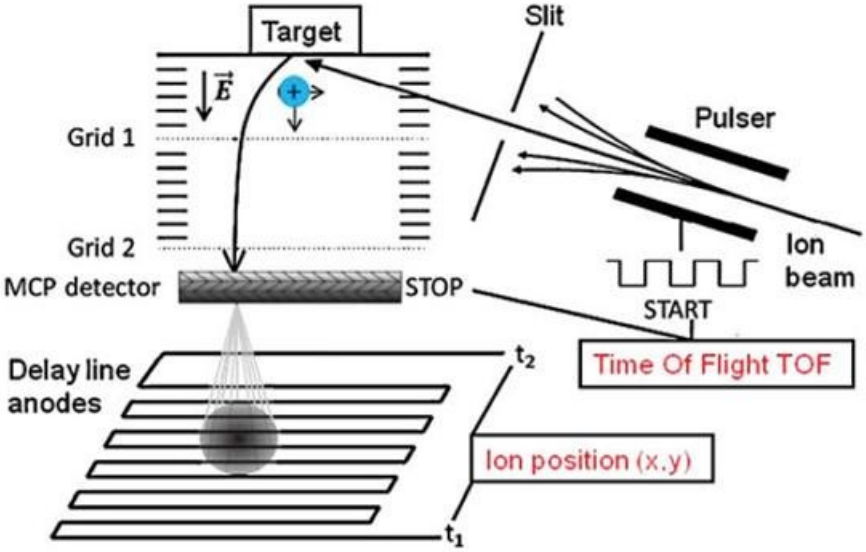


Figure 1. Schematic view of the experimental apparatus.

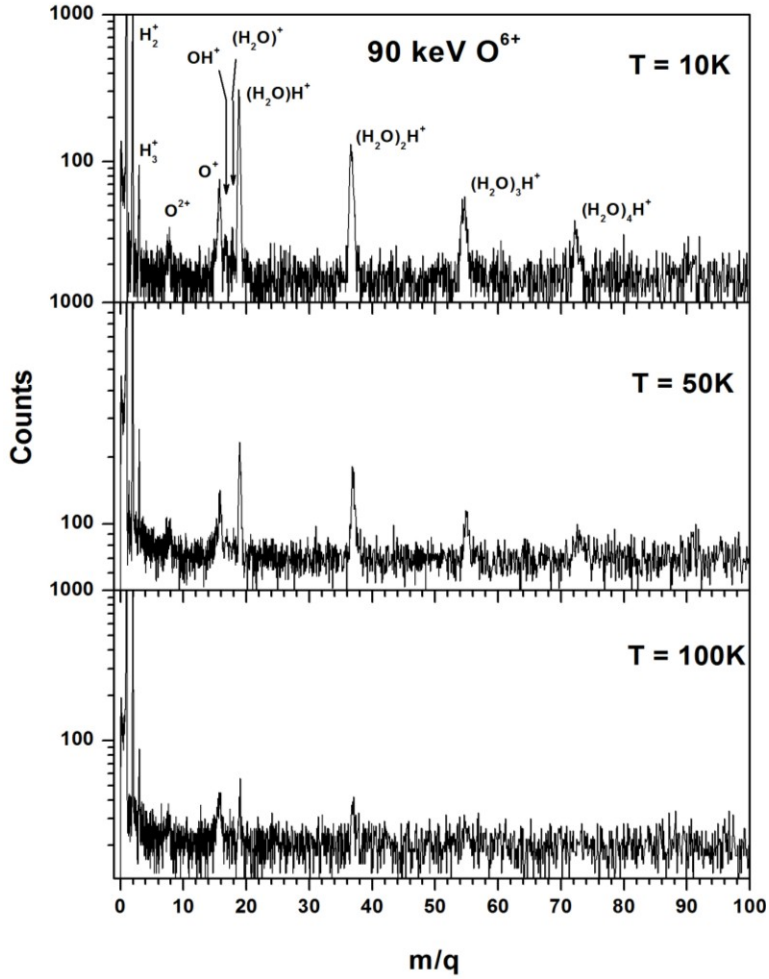


Figure 2. Mass spectra of secondary ions emitted from a water ice sample irradiated with 90 keV O^{6+} ions. The sample has been deposited at 10 K and then warmed up to 50 and 100 K.

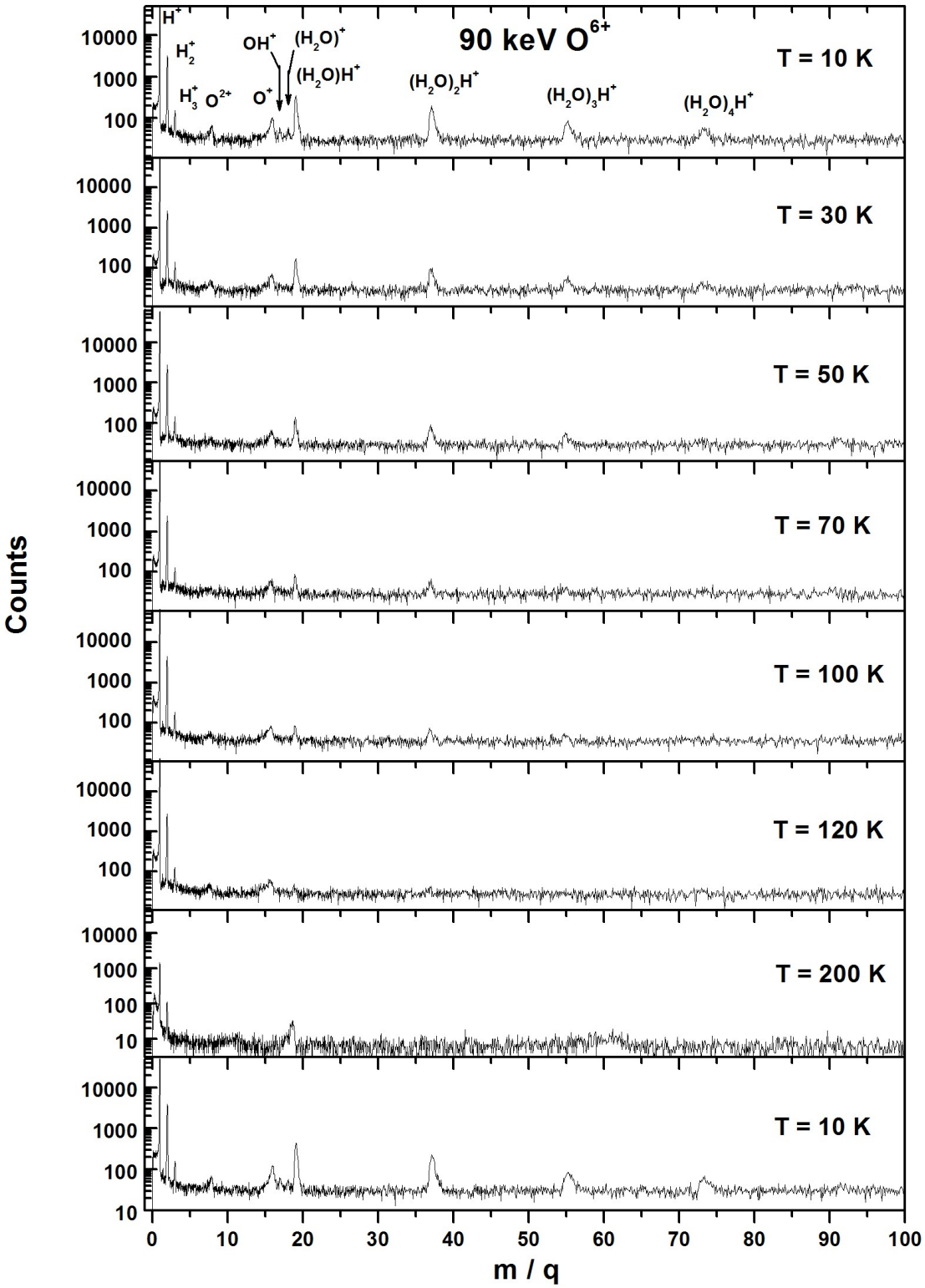


Figure 3. Mass spectra of secondary ions emitted from water ice samples irradiated with 90 keV O^{6+} ions. The sample has been initially deposited at 10 K; then fresh layers (always thicker than the penetration depth of the incoming ions) have been grown at each of the chosen temperatures.

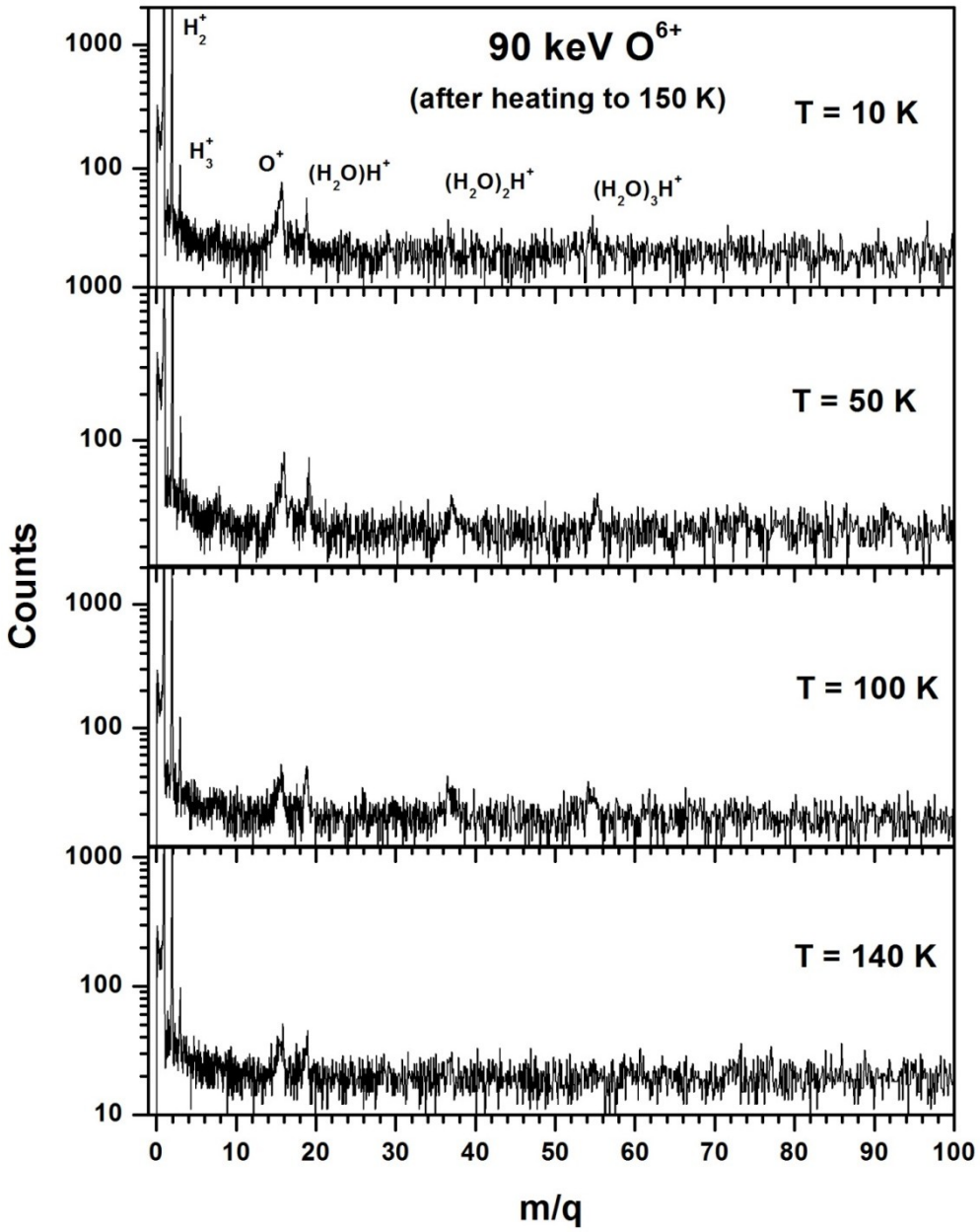


Figure 4. Mass spectra of secondary ions emitted from a water ice layer irradiated with 90 keV O^{6+} ions. The sample has been deposited at 10 K, then warmed up to 150 K and cooled down again to obtain a crystalline ice at low T.

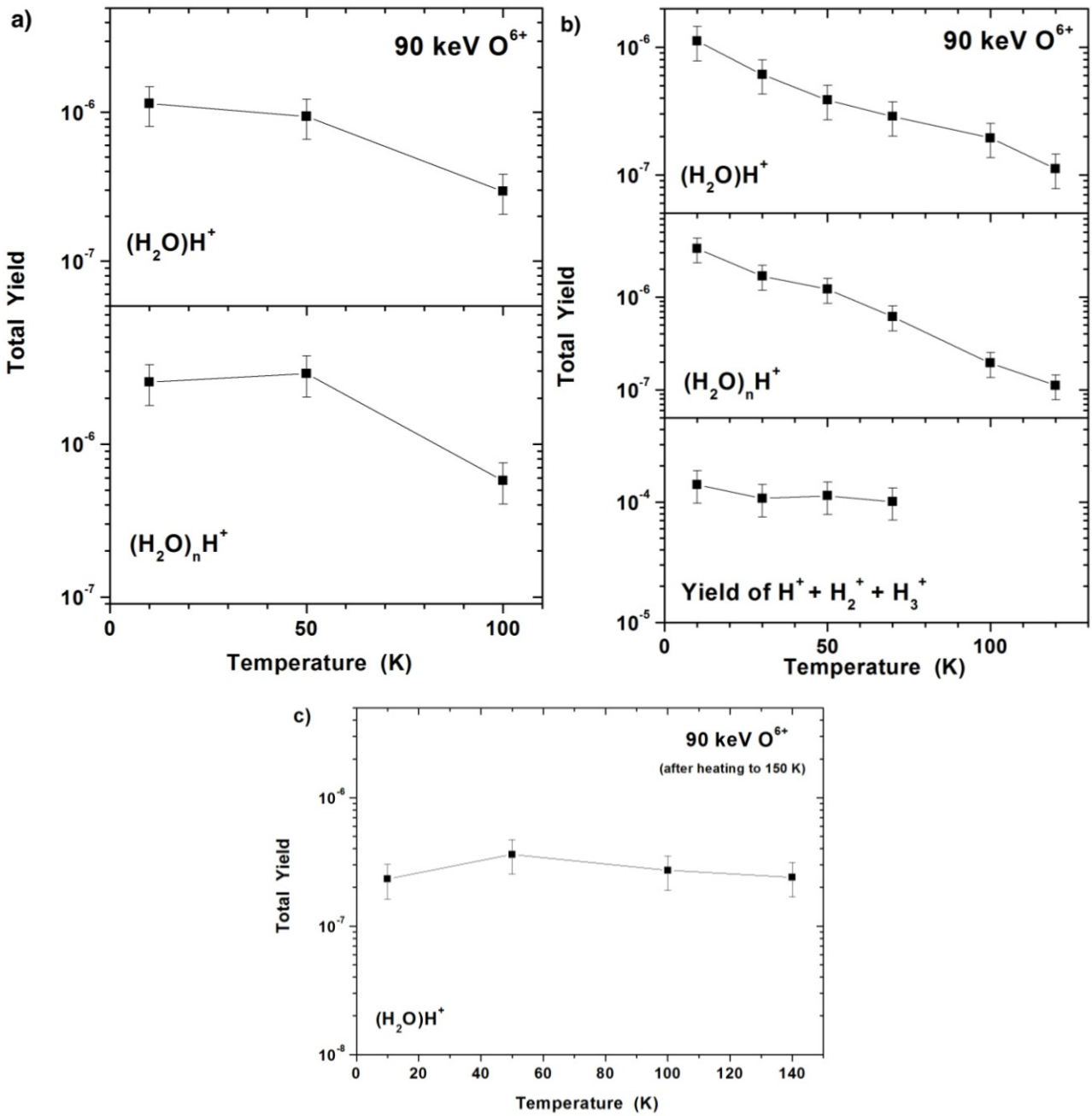


Figure 5. Secondary Total Ion Yields calculated for the most abundant secondary ion $(H_3O)^+$, for the total amount of clusters $(H_2O)_nH^+$ (n=1-8) and for the hydrogen ions (H^+, H_2^+, H_3^+); emitted from: a) amorphous ice water, b) fresh ice and c) crystalline ice water.

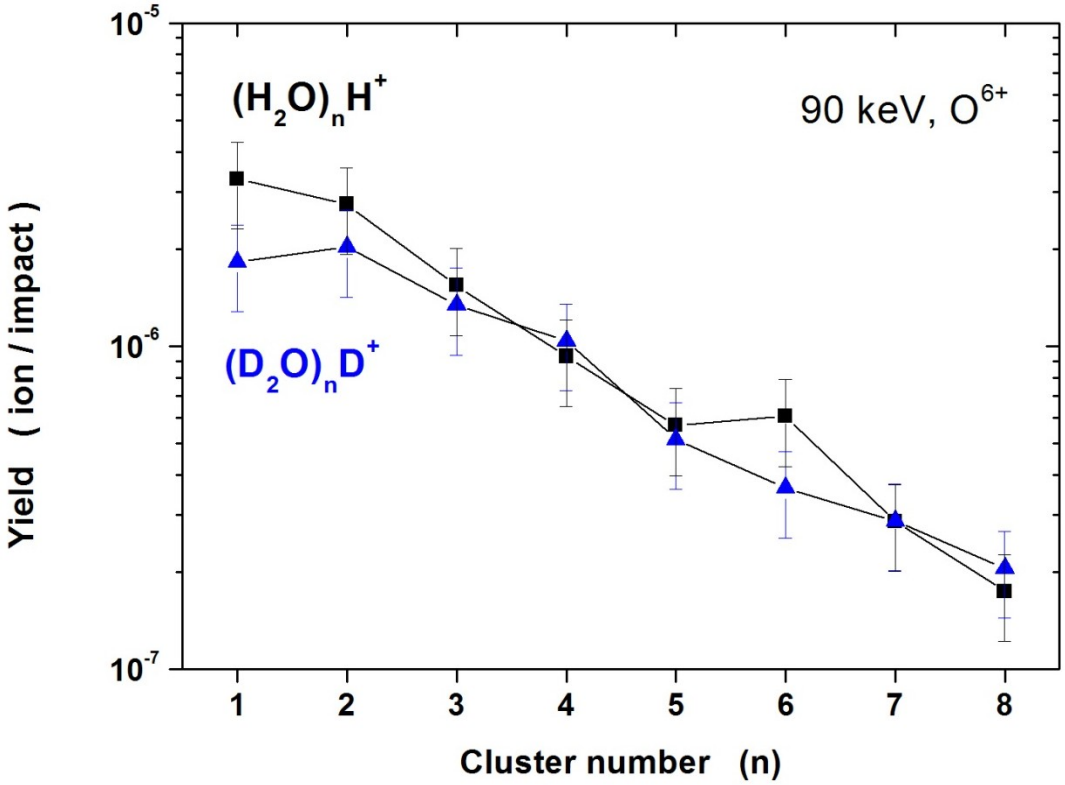
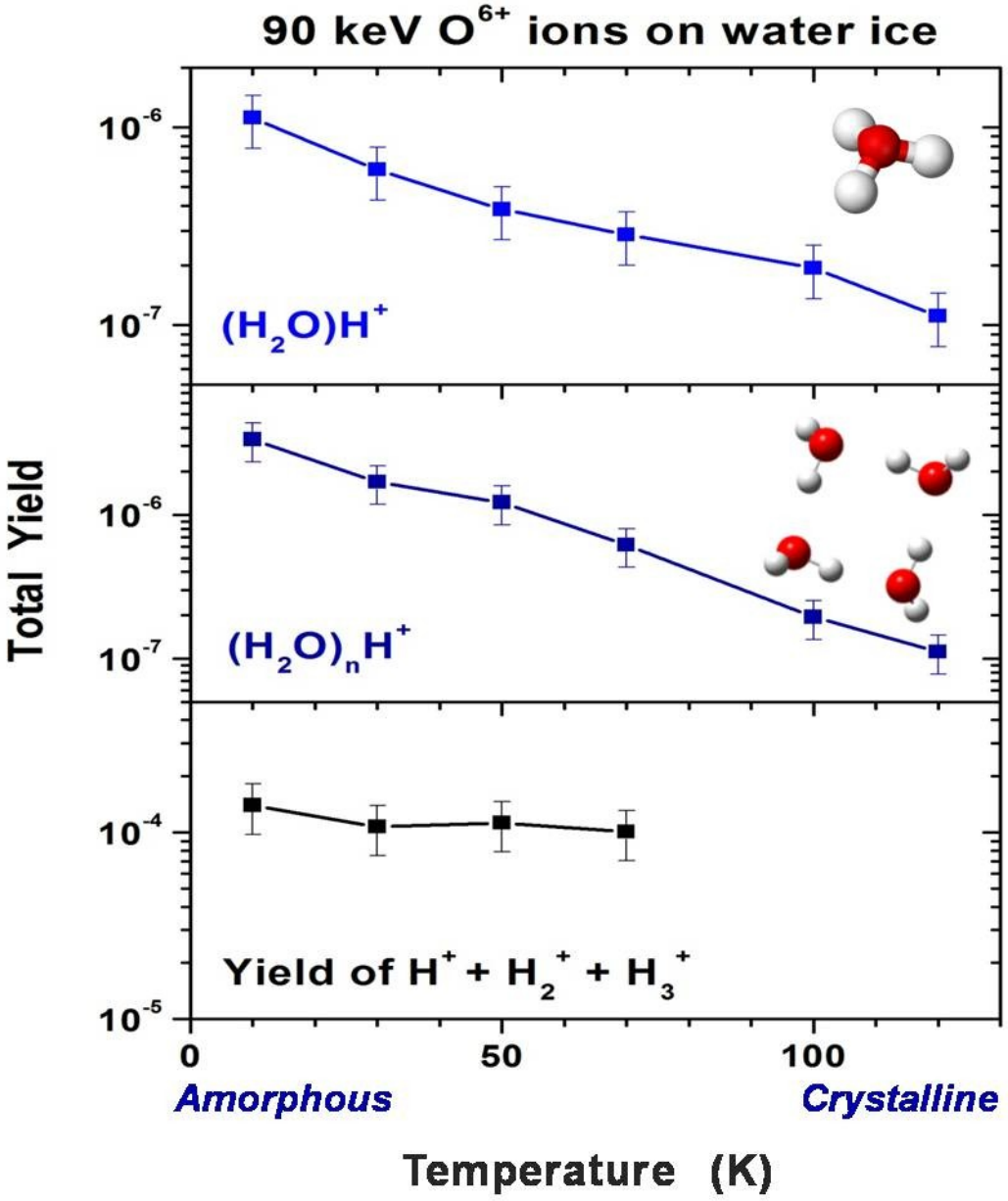


Figure 6. Secondary Total Ion Yields of $(H_2O)_nH^+$ and $(D_2O)_nD^+$ clusters (with n=1-8) emitted from water and deuterated water respectively. Both samples have been deposited and irradiated at 10 K.

TOC Image


90 keV O6+ ions on water ice
Total Yield
10-6
10-7
(H2O)H+
10-6
10-7
(H2O)nH+
10-4
10-5
Yield of H+ + H2+ + H3+
0
50
100
Amorphous
Crystalline
Temperature (K)